Physics
Cole Memorial Library

SCIENCE OF LIGHT

VOLUME 6 NUMBER 1

March

1957

OHIO STATE
UNIVERSITY
MAR 11 1958
LIBRARY

Published by the

Institute for Optical Research

Tokyo University of Education

in collaboration with

The Spectroscopical Society of Japan

SCIENCE OF LIGHT

Science of Light contains reports of the Institute for Optical Research and contributions from other science bodies about similar subjects.

The editorial staff consists of following members:

Chairman: Prof. H. Ootsuka, *Tokyo University of Education*

Dr. Y. Fujioka, *Atomic Energy Commission of Japan*

Prof. E. Minami, *Tokyo University*

Prof. M. Seya, *Tokyo University of Education*

Prof. Y. Uchida, *Kyoto University*

Prof. T. Uemura, *Rikkyo University*

Prof. K. Miyake, *Tokyo University of Education*

All communications should be addressed to the director or to the librarian of the Institute.

The Institute for Optical Research

Tokyo University of Education

400, 4-chome, Hyakunin-machi, Sinjuku-ku, Tokyo, Japan

Printed at
Kokusai Bunken Insatsusha
Chiyoda-ku, Tokyo.

Optical Properties of Thin Films of Al, Ag and Cu in Infrared Region

Keiei KUDO
Institute for Optical Research, Tokyo University of Education

Sanzo TAKEZAWA
Graduate course, Tokyo University of Education

(Received Feb. 10, 1957)

Abstract

The reflectance and transmittance of evaporated thin films of Al, Ag and Cu are measured in the region of wavelength from 1 to 15μ. Critical thickness found by Oppenheim and Scott is observed as about 60 A for Ag, Cu and 50 A for Al. The value for Ag is consistent with the value by Oppenheim. Extinction coefficients for metals are calculated using reflectance and transmittance and these values are compared with those given by Drude theory. In order to use the evaporated film of Al or Ag as infrared reflecting mirror it is necessary to make the layer thicker than 500 A.

1. Indroduction

Structures of thin film of metals were studied by many workers on electron microscope photographs[1)2)], by electron diffraction[3)4)5)] and by measuring the variation of resistance of the film[6)7)8)]. Thin films of almost all metals are known to consist of aggregation of particles, and it has been found that the state of the aggregation is different by the speed of evaporation of materials and that the particles begin to join together with neighbouring particles with increasing thickness. Hence, the reflectance and transmittance of thin film of metals are expected to be different from the values for bulk metals by the thickness and the speed of evaporation. This was verified experimentally in the visible region by Sennett and Scott[2)] using various metal films. Many methods have been employed for

1) H. Levinstein: J. App. Phys. **20** (1949) 306.
2) R.S. Sennett and Scott: J. Opt. Soc. Amer. **40** (1950) 203.
3) A.G. Quarell: Proc. Phys. Soc. (London) **49** (1937) 279.
4) L.H. Germer: Phys. Rev. **56** (1939) 58.
5) W. Latmor: Helv. Phys. Acta. **20** (1947) 441.
6) W. Reinders and L. Hamburger: Ann Physik **10** (1931) 649.
7) J. Porel: Helv Phys. Acta **24** (1951) 389.
8) C.E. Ells and G.D. Scott: J. App. Phys. **23** (1952) 31.

the determination of refractive index η and extinction coefficient κ of bulk metals, for example, the graphical method by Simson[9], the polarization method by Taylor[10], and the method by measuring the phase shift caused by interference or other method by Schulz[11][12]. Especially, Schulz's values are in good agreement with the computed values using Drude's metal theory[13]. For the structure of such films, Garnett'[14] introduced the rate of volume occupied by the metal particles in unit volume and formulated the relation of η and κ to the effective index of refraction η' and effective extinction coefficient κ'.

Study of optical properties of thin films has been made only in the region from ultraviolet to near infrared and left untouched in infrared region. On account of the weakness of source energy in infrared region, it is technically very difficult to examine the properties of thin films by interference. But by measuring the reflectance, transmittance and absorbance, determination of optical constants of Al, Ag and Cu in infrared region were made possible.

These measurements led to another study on the thickness of evaporated aluminium and silver films concerning their reflectance with the purpose of obtaining good reflectors for infrared work.

2. Experimental

Samples were prepared by deposition from vapor of source metals in a vacuum chamber of about 10^{-5} mmHg on rocksalt plate, polished optically flat and plane parallel. In order to eliminate the change in reflectance or transmittance due to the evaporation speed, five substrates were placed in a row in the chamber and the time of deposition was adjusted by a shutter placed between the vapor source and substrates.

For the measurement of reflectance, it is common to use substrates of a few degrees off parallel between the front and rear surfaces to eliminate the reflection on the rear surface, but such substrates are unsuitable for the measurement of transmittance. Therefore, as preliminary comparison test, reflectance was measured using wedge and parallel substrates. The difference in reflectances thus found was satisfactorily explained by taking into occount multiple reflections between the front and rear surfaces which enabled corrections to be made to

9) I. Simson: J. Opt. Soc. Amer. **41** (1951) 336.
10) J.E. Archard, P.Z. Cleggand and A.M. Taylor: Proc. Phys. Soc. **B65** (1952) 758.
11) L.G. Schulz: J. Opt. Soc. Amer. **41** (1951) 1047.
12) L.G. Schulz: J. Opt. Soc. Amer. **44** (1954) 540.
13) F. Seitz: The Modern theory of Solids Chapt. XVII.
14) J.C.M. Garnett: Trans. Roy. Soc. (London) **203A** (1904) 385.

observed values of reflectance using plane parallel substrates. The thickness of films was determined using Tolansky's method[15].

The measurements of reflectance and transmittance were made in infrared region from 1 to 15μ with a double beam double pass infrared spectrophotometer[16]. The error of measurement was $\pm\frac{1}{2}$ percent. For the transmittance measuremt, a rocksalt plate similar to the substrate of the sample was placed in the reference beam as shown in Fig. 1. For the reflectance measurement, a mirror M_1 was replaced by the sample. M_1' is a reference reflector, sufficiently aluminazed by evaporation, the reflectance of which was determined by the following procedure. First, the intensity of reflected beam by M_1' was measured. Then by displacing the light source to S' and taking M_1' away from the light path, the intensity of direct beam was measured. Incident angle of light to M_1 and M_1' was about 16°. The reflectance R_r of M_1', the standard reflector, was obtained as the ratio of the two measured values as shown in Table 1.

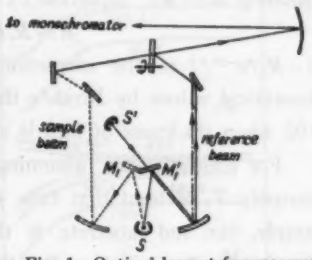

Fig. 1 Optical layout for measuring transmittance and reflectance.

Table 1. Reflectance R_r of standard aluminized reflector M_1'.

$\lambda(\mu)$	1	2	3	4	5	6	7	8	9	10	11	13	14	15
$R_r(\%)$	75	80	88	91	94	95	96	97	97	97	97	97	97	97

3. Preliminary consideration

Observed values of the transmittance T and the reflectance R on samples are not ture values. They necessitate corrections to be made.

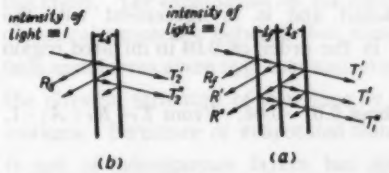

Fig. 2 Schematic diagrams showing the multiple transmission and reflection.
(a) film-substrate, (b) substrate only

For reflectance, as shown in Fig. 2 (a), the sum of reflection by front surface of film R_f, reflection on the boundary surface of film-substrate and reflection on the rear surface of substrate is measured. Assuming that the intensity of incident light is unity, reflection R_{rec} recorded is written by the following equation

15) L.G.S. Tolansky: Multiple Beam Interferometry (Oxford University Press, New York, 1948), p. 147.
16) K. Kudo: Science of Light, **5** (1956) 89.

$$R_{rec}=\left(\frac{1}{R_r}\right)(R_f+R'+R''+\ldots.)$$
$$=\left(\frac{1}{R_r}\right)\{R_f+(1-R_f)^2R_{f,s}e^{-2\alpha_f t_f}+(1-R_f)^2(1-R_{f,s})^2R_s e^{-(2\alpha_f t_f+\alpha_s t_s)}+\ldots.\}, \quad (1)$$

where, R, α and t are reflectance, absorption coefficient and thickness respectively, and subscripts r, f and s are affixed to the reference reflector, film and substrate respectively. Effect of the third and further terms will be very small and approximately $R_{fs}=R_f$. Equation (1) is then simplified as

$$R_f=R_rR_{rec}\{1-(1-R_f)^2e^{-2\alpha_f t_f}\}. \quad (2)$$

$(1-R_f)^2e^{-2\alpha_f t_f}$ is the correction term, and if R_{rec} is used instead of R_f the theoretical values by Drude's theory for α_f, $(1-R_{rec})^2e^{-2\alpha_f t_f}$ becomes about 0.08–0.02 when thickness of film is about 100 A.

For transmittance, assuming that the intensity of incident light is unity, the intensity T_1 of light that falls on the monochromator after passing through the sample, film and substrate is the sum of T_1', T_1'', T_1''' and so on as shown in Fig. 2 (a). By assuming $R_f=R_{fs}$, transmittance T_f of the film is written as

$$T_f=(1-R_f)^2e^{-\alpha_f t_f}. \quad (3)$$

Hence,

$$T_1=T_f(1-R_s)e^{-\alpha_s t_s}\{1+R_{f,s}R_s e^{-2\alpha_s t_s}+R_fR_{f,s}e^{-2\alpha_f t_f}+\ldots.\}. \quad (4)$$

Since a plane parellel rocksalt plate is placed in reference beam, the intensity of light that falls on the monochromator in the reference beam side is, as seen from Fig. 2 (b),

$$T_2=T'+T''\ldots.$$
$$=(1-R_s)^2e^{-\alpha_s t_s}(1+R_s^2e^{-2\alpha_s t_s}). \quad (5)$$

The transmittance T_{rec} recorded by the spectrophotometer is T_1/T_2. Assuming that $\alpha_s=0$, $R_{fs}=R_f$ and $R_s\ll 1$,

$$T_f=T_{rec}\{1-R_s(1+R_f)\}. \quad (6)$$

Since $R_s(1-R_f)$ is also the correction term, R_{rec} can be used instead of R_f. R_s is determined by observation as already mentioned, and is in agreement with the result of calculation. The value of R_s was in the order of 0.04 in infrared region from 1 to 15μ.

The correction term in Equation (6) is about 0.07–0.04. From $T_f+R_f+A_f=1$, the absorbance A_f is obtained.

4. Optical properties

By correcting the recorded data with the method mentioned above, the transmittance and reflectance of thin films of Al, Ag and Cu with various thicknesses were obtained respectively as shown in Figs. 3 (a) and (b) in the region from 1

to 15μ. The features of t *vs* A_f, T_f and R_f are plotted in Figs. 4 and 5. As clearly

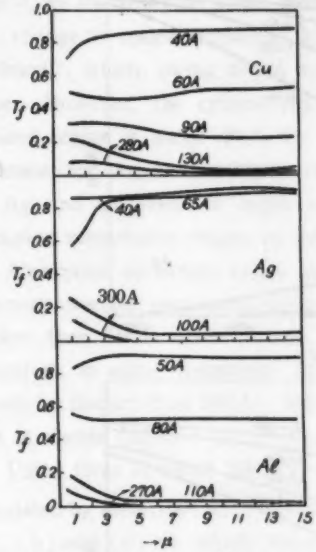

Fig. 3 (a) Transmittances T_f of Al, Ag and Cu.

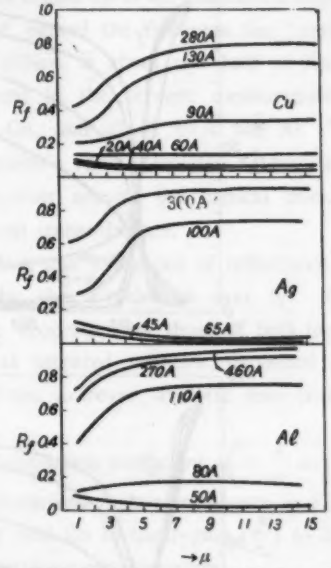

Fig. 3 (b) Reflectances R_f of Al, Ag and Cu.

shown in Figs. 4 and 5 that A_f, R_f and T_f vary remarkably by the thickness from 50 to 100 A. As seen in Fig. 4, the absorbance maxima of Al, Ag and Cu films are at about 100 A. Hence, we can expect that the evaporated thin film of metals show a structural change within the above range of thickness. The explanation for the difference of optical properties between thin films and bulk metals was given by a thorough study on the physical structure of thin films by many workers. Structure of evaporated thin films is not of homogenous layers but spongy. Moreover, "*very*" thin films of metal consist of aggragates of the metal particles. With increasing thickness, its structure becomes similar to that of homogenous layer. Result above mentioned in the visible region and

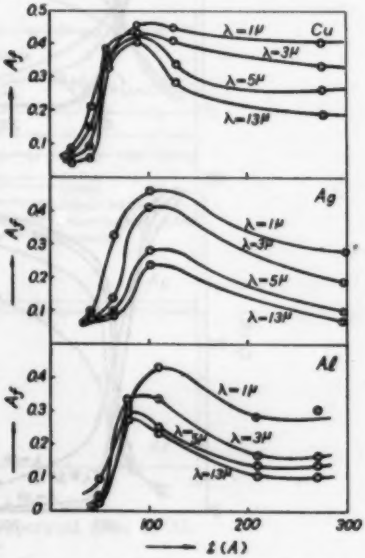

Fig. 4 Graphs showing absorbance A_f *vs* film thickness t.

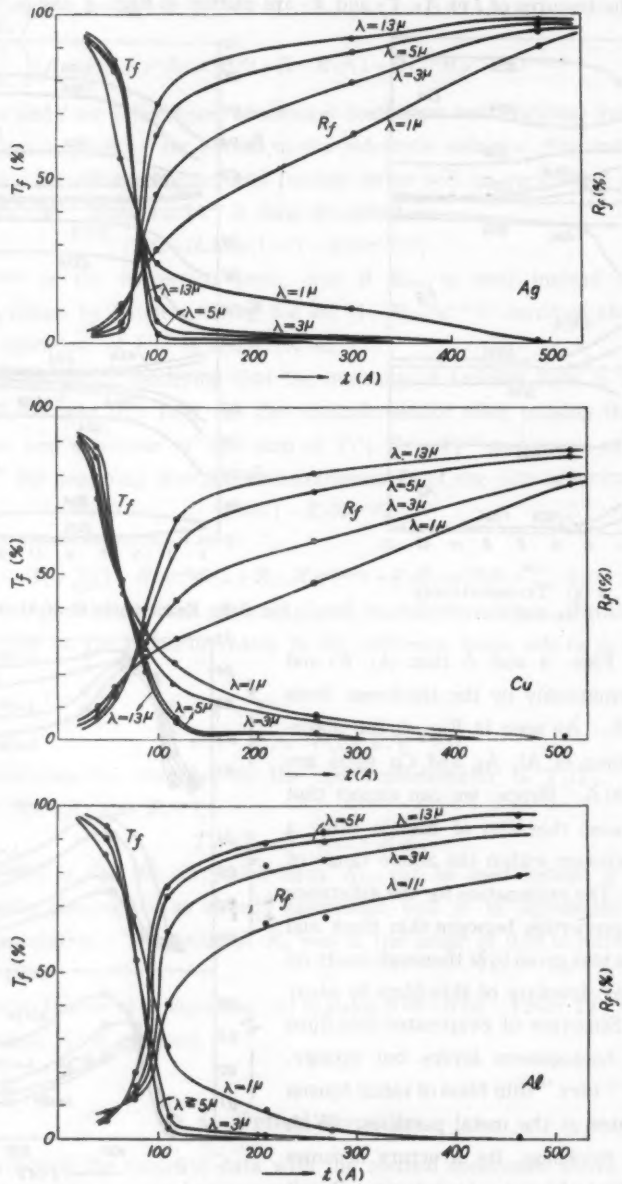

Fig. 5 Graphs showing transmittance T_f and reflectance R_f *vs* thickness t.

in the study of structure supports the authors' data in infrared region. Oppenheim[17], by the study on silver thin film in the region up to 4μ, observed a remarkable change in optical properties at 60 A and named the thickness the "***critical thickness***", which, owing to yet unrevealed reason is about one half of Scott's value. However, the critical thickness found in the present measurement in infrared region is about 60 A for Ag and Cu, and about 50 A for Al. This thickness for Ag is consistent with Oppenheim's value. Isolated aggregates of Al, Ag and Cu seem to begin joining together around the critical thickness disclosing remarkable chages in reflectance and transmittance.

Absorption maximum exists at about 100 A and variations of reflectance and transmittance are very small beyond 100 A for the wavelength over 5μ. Films thicker than 500 A show almost the same properties as those of bulk metals. Therefore, in using evaporated Al or Ag as infrared reflector, deposited films should be thicker than 500 A. 500 A thick films, however, are still semi-transparent in visible region.

Using films of about 100 A in thickness, extinction coefficient $\kappa\left(=\frac{\lambda}{4\pi}\alpha_f\right)$ was calculated by Equation (3). Values of κ/λ for various metals are shown in Figs. 6 (a), (b) and (c) in which values for Ag and Cu in the region of 1 to 3μ by

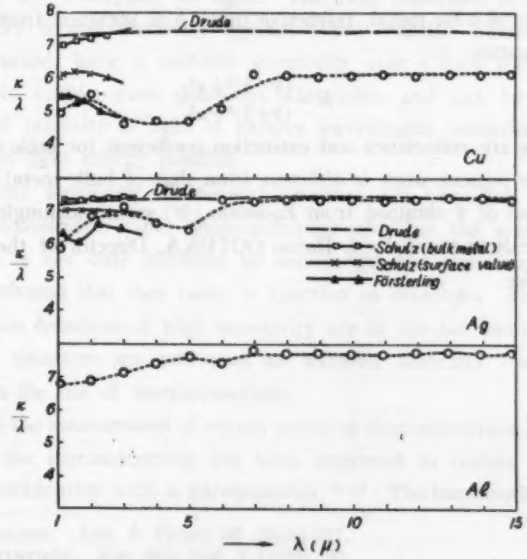

Fig. 6 Graphs showin κ/λ for evaporated films of Al, Ag and Cu.

17) U. Oppenheim: J. Opt. Soc. Amer. **46** (1956) 628.

Schultz[13] and Forsterling[18] are plotted for comparison. The dashed curves with "Drude" were obtained by calculation using the equations

$$\eta^2-\kappa^2=1-2\left(\frac{Ne^2}{2\pi m^*}\right)\frac{1}{\gamma^2+\nu^2}, \tag{7}$$

$$\eta\kappa=\frac{\gamma}{\nu}\left(\frac{Ne^2}{2\pi m^*}\right)\frac{1}{\gamma^2+\nu^2}, \tag{8}$$

where, $\gamma=\left(\frac{Ne^2}{2\pi m^*}\right)\frac{1}{\sigma}$ and e is the charge of the electron and m^* its effective mass, N the number of free electrons per unit volume, σ the conductivity of the metal and ν is the frequency of radiation. The authors' values of κ/λ for Ag and Cu are somewhat small in comparison with Schulz's values in the wavelength up to 3μ. Likely explanation of this difference is that Schulz's values are for layers thicker than the authers' and the latter's values correspond to the effective extinction coefficient κ' in Garnett's theory. But, since the reflectance and transmittance in the wavelength beyond 5μ remain almost unchanged for increasing wavelength, κ in long wave region will be close to the values of bulk metals. The error in κ is comparatively large (about 10%); it is chiefly caused by the inaccuracy of the measurement of thickness by Tolansky's method and by the considerable influence of small erreors in T_{rco} and R_{rco} on the calculated values of κ.

In the case of bulk metal, refractive index η is obtained from the following well-known equation,

$$R=\frac{(\eta-1)^2+\kappa^2}{(\eta+1)^2+\kappa^2}, \tag{9}$$

where R and κ are reflectance and extinction coefficient for bulk metal. Since κ obtained in the present work is different from that of bulk metal even for thick films, the values of η obtained from Equation (9) seem meaningless.

Authors wish to thank Prof. Haruo OOTUKA, Director of the Institute, for his useful abvice.

18) K. Forsterling and V. Freedericksz, Ann. Phys. **40** (1913) 201.

On the Thermojunction for A. C. Use

Masatoshi NAKAMURA

Institute for Optical Research, Tokyo University of Education

(Received Jan. 15, 1957)

Abstract

Characteristics of thermojunctions produced using old technique is investigated. As the thermoelectric material, B_i–S_b and S_b–C_d alloys are used and the receivers are made with gold foil blackened by gold-black. The d. c. voltage sensitivity ϵ_∞, time constant τ, characteristic a. c. voltage sensitivity $S_{a.c}=\epsilon_\infty R^{-\frac{1}{2}}[1+\omega^2\tau^2]^{-\frac{1}{2}}$ etc. are studied as functions of the length of thermoelectric wires. Wires of various lengths and diameters are used and the time constant of the thermojunction of the shortest length of wires used (l=0.15 mm) was 0.01 sec. in air and 0.025 sec. in vacuum.

1. Introduction

Thermojunctions are used as thermal detecters along with bolometer, thermister bolometer etc. which measure the light intensity utilizing the elevation of temperature by the absorption of light. The most important property of these thermal detectors is non-selectivity against wave length. Thermojunctions, if properly constructed, have a uniform sensitivity over a wide wavelength range from infrared to visible, even down to ultraviolet, and can be used for the measurement of intensity of light of various wavelengths rendering the absolute measurements of light energy possible.

Generally, the sensitivity of thermal detectors are very low in comparison with that of photoelectric tube, photo-multiplier etc. but the sensitivity of the latter detectors is not only different by wavelength but also becomes so low in the region of infrared that they cease to function as detectors. Recently various kinds of radiation detectors of high sensitivity are in use but owing to the above reason thermal detectors are still used as infrared detectors fostering further developement in the use of thermojunctions.

Formerly in the measurenent of output power of thermojunction, galvanometers were used and the thermojunction has been improved to realize the maximum sensitivity in combination with a galvanometer.[1)-4)] The thermopile was invented

1) E. S. Johansen: Ann. d. Physik **33** (1910) 517.
2) C. H. Cartwright: Rev. Sci. Inst. **1** (1930) 592.
3) F. A. Firestone: Rev. Sci. Inst. **1** (1930) 630.
4) J. Strong: Rev. Sci. Inst. **3** (1932) 65.

in which many thermojunctions are connected in series or parallel. The response time of a thermopile or a thermojunction was considered to be not so important in these thermopile- or thermojunction-galvanometer systems because it is limited by the period of galvanometer.

After the Second World War, amplifying method of the output power of a thermojunction using electric tube has come widely into use. There are two methods in amplifying. One is the d. c. amplifying method in which an electric tube replaces the galvanometer. The other is the a. c. amplifying method in which chopped light is received by a thermojunction and the a. c. output power is amplified. In the latter method only a. c. signals are amplified eliminating zero drift which is an important problem in the cases of d. c. amplifying and galvanometer methods. Adding to this, recent progress in amplification of signals by very low frequency such as a few cycles per second has made the a. c. amplifying method to be used in most cases. But for adopting the a. c. amplifying method, the thermojunction must have a fast response for which the study of thermojunction has been directed to a new field.

Harris and Scholp[5] developed a technique of making thermojunctions or thermopiles with thin film of thermoelectric materials by evaporation and succeeded to obtain fast response. Ross and Dacuss[6] also made thermojunctions for a. c. use by evaporation method and thereafter the vacuum evaporation method has been used by many investigators[7].

Schwarz[8] and Liston[9] independently succeeded in producing a special form of fast response thermojunction by using semiconducting wires of strong electromotive force, thick enough—about 1 mm—to be of small resistance. To reduce the effective heat capacity, Schwarz sharpened the end of the wire like a pin and Liston like a knife edge.

Hornig and O'Keefe[10] determined the factor of merit for thermoelectric materials and gave the design criteria for maximum sensitivity and fast response of thermopiles produced by old technique.

In the design of thermojunction with given thermoelectric materiales, the form of the thermo junction is decided by the following factors, namely the heat loss from hot junction, heat capacity of hot junction and total resistance of thermojunction.

5) L. Harris and A. C. Scholp: Jur. Opt. Soc. Amer. **30** (1940) 519.
6) L. C. Ross and E. N. Dacuss: Rev. Sci. Inst. **16** (1945) 164.
7) T. Sakurai, K. Kanaya and K. Shishido: Sci. Rep. Res. Inst. Tohoku Univ. **A1** (1949) 313.
8) E. Schwarz: British Patent Specification, 578, 187, 578, 188.
9) M. D. Liston: Jur. Opt. Soc. Amer., **37** (1947) 515.
10) D. F. Hornig and B. J. O'Keefe: Rev. Sci. Inst., **18** (1947) 479.

The auther, in preparing thermojunction of fast response, adopted the old technique recommended by Hornig and O'Keefe, namely, the wires were made by Taylar's method[11] and the thermojunctions were prepared using these wires. Materiales used were B_i-S_b and S_b-C_d alloys. Gold foil of 0.5μ in thickness was used for the light receiving surface of $0.4\times1.5\,mm^2$, which was blackened with gold-black.

2. Equilibrium (D. C.) Voltage Sensitivity

If the blackend receiver of a thermojunction is exposed to a radiation flux P, the e. m. f. generated in the thermojunction with thermoelectric power K, at any time t after the illumination is given by

$$E=E_\infty\left[1-\exp\left(-\frac{t}{\tau}\right)\right], \tag{1}$$

where $E_\infty=\dfrac{KP}{L}$ is the equilibrium thermoelectro motive force and τ is the time constant which is expressed by

$$\tau=\frac{C}{L}. \tag{2}$$

In this equation L is the total heat loss to the surroundings per second per degree of temperature difference and it is considered that L is the sum of the heat losses by radiation L_r, by wire conduction L_w and by convection of gas L_g. C is the effective heat capacity of the hot junction consisting of the total heat capacity of the receiver and a part of the heat capacity of the wires.

If the equilibrium (d. c.) voltage sensitivity of thermojunction is defined as the equilibrium e. m. f. (μV) generated per unit radiant energy (μW) incident upon the receiver, following equation may be obtained

$$\varepsilon_\infty=\frac{E_\infty}{P}=\frac{K}{L}=K[L_r+L_w+L_g]^{-1} \tag{3}$$

As L_w is the heat loss by wire conduction per second per degree of temperature difference, if the two wire materials are marked by subscripts 1 and 2, then

$$L_w=k_1\left(\frac{s_1}{l_1}\right)+k_2\left(\frac{s_2}{l_2}\right) \tag{4}$$

for a single junction, where k is the thermal conductivity of the wire material, s the cross-sectional area of the wire and l the length of the wire.

If the wire dimensions are chosen from the optimum relation first found by Johansen[1],

$$\left(\frac{s_1}{l_1}\right)^2\frac{k_1}{\rho_1}=\left(\frac{s_2}{l_2}\right)^2\frac{k_2}{\rho_2} \tag{5}$$

11) J. Strong: Procedures in Experimental Physics (1939) Chapter 8.

where ρ is the specific resistance of the wire material, and if the lengths of the two wires are set equal to l, then Equation (4) may be written

$$L_w = \frac{\pi k_1}{4}\left\{1+\left(\frac{k_2\rho_2}{k_1\rho_1}\right)^{\frac{1}{2}}\right\}\frac{a_1^2}{l} \qquad (6)$$

where a_1 is the diamter of one of the wires of the couple. Now if the casing of the thermojunction is evacuated, then L_σ tends to zero and in addition if the relation $L_r \ll L_w$ is assumed, then ε_∞ becomes proportional to l for given a_1 (or a_2).

Measurement of ε_∞ has been made using a voltage sensitive galvanometer of the sensitivity of 5×10^{-8} volts/mm and a standard electric lamp, the characteristics of which are as follows: applied voltage, 90.3 volts; filament current, 0.351 amperes; color temperture, 2355°C; radiation density at one meter from the lamp, 299 μw/cm^2. Wire diameters of 10μ, 30μ and 50μ were chosen for a_1, and ε_∞ was measured first under atmospheric pressure and then after evacuation by varying a_1 and l.

A glass plate was used for the entrance window of the thermojunction casing.

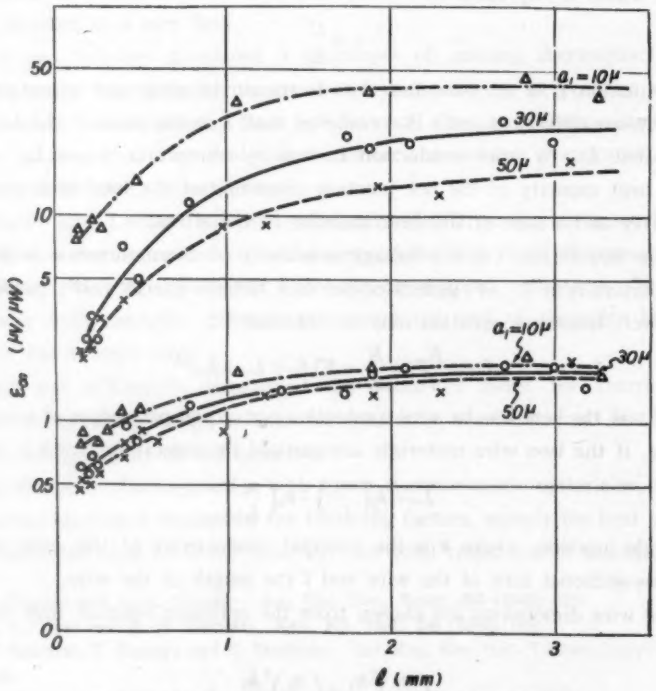

Fig. 1 Equilibrium voltage sensitivity *vs* wire length.
Three curves of the lower group were obtained under atmospheric pressure and three curves of the upper group in vacuum.

Loss of light caused by reflection at the glass surface and absorption by the glass plate was previously measured which was, in all, 33% of the light. Taking this loss into consideration, the sensitivity of evacuated themojunctions were measured. The results obtained are shown in Fig. 1, in which three curves of the lower group are by the observation under atmospheric pressure and three curves of the upper group are after evacuation. In the figure, it is seen that, as reasoned above, ε_∞ is nearly proprtional to l for small l (below about 1.5 mm) except for $a_1=10\mu$, under evacuated condition. This proportionality, however, does not hold for large l. It seems to show that as l increase, that is, as L_w decrease, L_r becomes effective in L. This may be perceived likewise in the case of $a_1=10\mu$. It is natural from the dependency of L upon a_1 under atmospheric pressure as well as evacuated condition that, as a_1 decreases, ε_∞ increases for the same l (curves are raised). In the case under atmospheric pressure, however, the increase of ε_∞ are not so conspicuous. This is probably due to the great contribution of L_g to L.

3. Time Constant

When a thermojunction is exposed to radiation which is chopped to make square wave signals of frequency f c. p. s. (the radiation in the spectrometer usually has the form of square waves), the amplitude of oscillating thermo e. m. f. induced in the thermojunction is expressed by the following formula

$$\varepsilon=\frac{\varepsilon_\infty}{2}\tanh\left(\frac{1}{4\tau f}\right) \tag{7}$$

In the case when this oscillating output signal is amplified by an amplifier tuned to the chopping frequency, merely the fundamental frequency of the square waves is sufficient to be taken into account, which leads the expressoin of the amplitude (r. m. s.) to the following equation.

$$\varepsilon_{a.c}=\frac{\sqrt{2}}{\pi}\frac{\varepsilon_\infty}{(1+\omega^2\tau^2)^{1/2}},\qquad \omega=2\pi f. \tag{8}$$

This $\varepsilon_{a.c}$ given by Equation (8) should be considered in the investigation of the response of thermojunction combined with a tuned amplifier. The values of the term $(1+\omega^2\tau^2)^{-\frac{1}{2}}$, which represents relative frequency response, are shown in Fig. 2 as a function of the time constant τ for $f=5$ c. p. s.

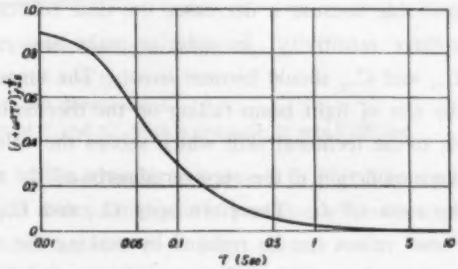

Fig. 2 Relative frequancy response *vs* time constant for $f=5$ c. p. s.

The time constant of thermo-

junction, τ, expressed in Equation (2), can be written in the following form.

$$\tau = \frac{C}{L} = \frac{C_f + C_b + C_{\omega 1} + C_{\omega 2}}{L_r + L_\omega + L_g} \tag{9}$$

where

$C_f = c_f A d_f$: heat capacity of the foil forming the receiver.
$C_b = c_b A d_b$: heat capacity of the black.
$C_{\omega 1} = c_{\omega 1} \alpha_1 s_1 l_1$: effective heat capacity of one wire.
$C_{\omega 2} = c_{\omega 2} \alpha_2 s_2 l_2$: effective heat capacity of the other wire.
c_f, c_b, c_ω : specific heats of the foil, black and wire.
A : area of the receiver.
d_f, d_b : thicknesses of the foil and the black.
α_1, α_2 : only α fraction of the hot junction assumed to contribute to the heat capacity.

According to this equation, there are two ways of reducing the value of τ, i. e., (1) by making L large and (2) by making C small. The former way will be considered at first. Suppose that a thermojunction is already made complete and also that L is possible to be changed without changing any other characteristics of the thermojunction, and examine how the amplitude $\varepsilon_{a.c}$ given by Equation (8) varies with the change of L. By differentiating $\varepsilon_{a.c}$ by L,

$$\frac{d\varepsilon_{a.c}}{dL} = -\frac{\sqrt{2}K}{\pi} \cdot \frac{L}{(L^2 + \omega^2 C^2)} \tag{10}$$

which indicates that $\varepsilon_{a.c}$ decreases as L increases. This leads to the conclusion hat if L alone can be reduced without affecting any other properties of the thermojunction, better response would be obtained in spite of the increase in the time constant. This is just the case when a thermojunction is used in vacuum. The effective heat capacity of the wires might, in reality, suffer a slight change by evacuation, which will be discussed later.

Next, the latter way of reducing τ is considered. The reduction of C is very desirable because it decreases the time constant without affecting the equilibrium voltage sensitivity. In order to make heat capacity small, each value of C_f, C_b, C_{ω_1} and C_{ω_2} should become small. The amounts of C_f and C_b are subjected to the size of light beam falling on the thermojunction which incidentally determines A, to the technical skill which settles the value of d_f and to the condition of the thermojunction if the receiver absorbs all the radiation incident upon it which gives the value of d_b. Therefore only C_{ω_1} and C_{ω_2} are left to be chosen arbitrarily. These values can be reduced by making the wires of thermojunction as fine and as short as possible. However the use of fine wire results in the increase of resistance and comes to the reduction of characteristic sensitivity which will be

discussed later and the shortness of the wire results in the increase of L_ω.

The influences of these factors on the properties of thermojunction were investigated by measuring the time constant for various values of l with given diameters of the wire.

Fig. 3 Schematic diagram of the apparatus used in the measurement of the time constants.
L: Lens
S: Shutter
T: Thermojunction
G: Element of an electromagnetic oscillograph
D: Recording drum

The measurement of the time constant was carried out by using the arrangement shown in Fig. 3. G is a D type element (sensitivity, 2μA/mm, period undamped, 3ms.) for an electromagnetic oscillograph made in Yokogawa Electric Work. The radiation from the source is focused on the thermojunction T by a lens L, in front of which a camera shutter S is provided. Opening and shutting of the shutter send the pulses of light beam on to the receiver of thermojunction. The response of the thermojunction is recorded on a printing paper on drum with the D type element.

The error of measurement of the time constant inherent in this arrangement was found to be 0.002~0.003 sec. by replacing the thermojunction with a photovoltaic cell. An example of the response curve obtained by this method is shown in Fig. 4. The time constant was determined from the response curves and

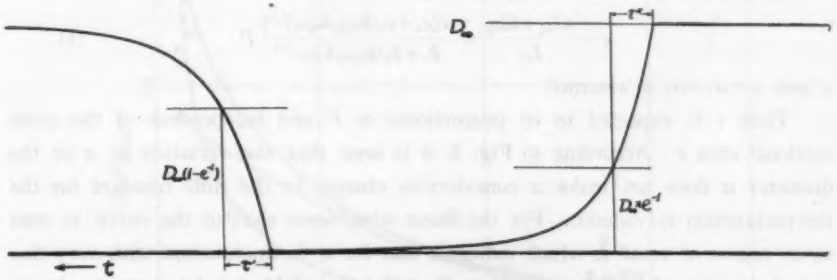

Fig. 4 Example of the electromagnetic oscillogram
τ' : Time constant obtained from the rise curve.
τ'': Time constant obtained from the decay curve.
τ was obtined by taking an average of τ' and τ'', in this example, it was 0.028 sec.

the rotating velocity of the drum. These results are shown in Fig. 5 in which the lower three curves were obtained under atmospheric pressure while the upper three curves in vacuum.

If a very thin foil is used to form the receiver and its area is made so small that the relation, $C_f+C_b \ll C_{\omega_1}+C_{\omega_2}$, is held and again, if the condition $L_g=0$ and

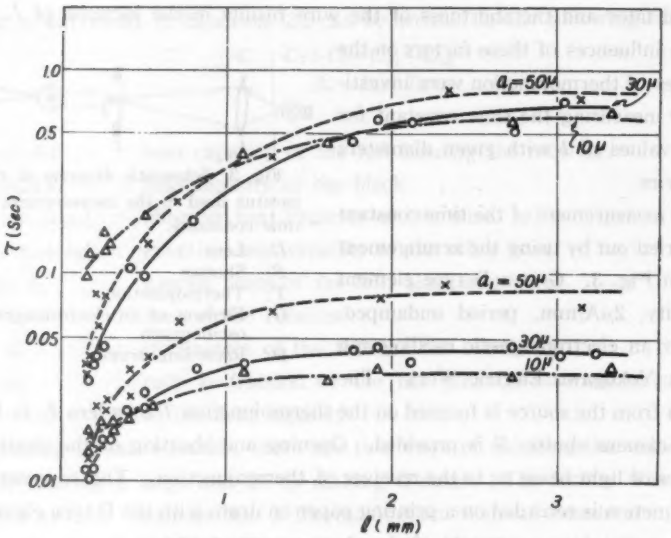

Fig. 5 Time constant *vs* wire length
Three curves of the lower group were obtained under atnospheric pressure and three curves of the upper group in vacuum.

$L_r \ll L_\omega$ for L are fulfilled as assumed previously in the discussion of the equilibrium voltage sensitivity, τ can be expressed as

$$\tau = \frac{C_{\omega_1}+C_{\omega_2}}{L_\omega} = \frac{\alpha\{c_1+c_2(k_1\rho_2/k_2\rho_1)^{1/2}\}}{k_1+k_2(k_1\rho_2/k_2\rho_1)^{1/2}} l^2 \tag{11}$$

where $\alpha=\alpha_1=\alpha_2$ is assumed.

Thus τ is expected to be proportional to l^2 and independent of the cross sectional area s. According to Fig. 5, it is seen that the variation of s or the diameter a does not make a considerable change in the time constant for the thermojunction in vacuum. For the finest wire, some shift of the curve is seen in the region of small l, which indicates that for a thermojunction with very fine and short wires the assumption $C_{\omega_1}+C_{\omega_2} \gg C_f+C_b$ might not be correct. Incorrectness of the assumption might also be the cause of the dependence of the time constant τ on l being different from what is expected from the relation derived above. For short l and large s, τ is proportional only to $l^{1.3\sim1.5}$ at best.

4. Characteristic A. C. Voltage Sensitivity

When a thermojunction is used in combination with an a. c. amplifier, the amplitude of its output is expressed by Equation (8). This amplitude will be called hereafter the a. c. voltage sensitivity. Further, we should be fully acquainted

with the intrinsic noise of the detector before we speak of its performance. The performance should be expressed in terms of minimum detectable power. We consider, as it said, the main source of the noise of a thermojunction is the Johnson noise. This noise is given by fhe well known formula

$$E_J(\text{r. m. s.}) = [4kTR\Delta f]^{\frac{1}{2}} \tag{12}$$

Then the minimum detectable power of a thermojunction is given by the following equation :

$$P_{\min} = [4kTR\Delta f]^{1/2}/\mathcal{E}_{a.c} = \frac{[4kT\Delta f]^{1/2} \cdot R^{1/2}\pi[1+\omega^2\tau^2]^{1/2}}{\sqrt{2}\,\mathcal{E}_\infty}$$

$$= [2kT\Delta f]^{1/2}\pi/S_{a.c} \tag{13}$$

where

$$S_{a.c} = \mathcal{E}_\infty/R^{1/2}[1+\omega^2\tau^2]^{1/2} \tag{14}$$

$S_{a.c}$ will be called the " characteristic a. c. voltage sensivity " in the following discussion.

Assuming that the thermojunction is used with a chopping frequency of 5 c. p. s., Fig. 6 was obtained by drawing $S_{a.c}$ verses l. The lower three curves

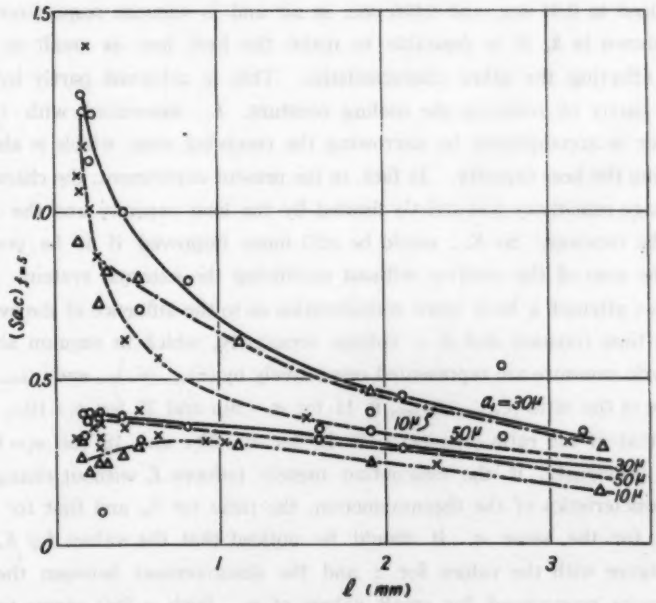

Fig. 6 Characteristic a. c. voltage sensitivity *vs* wire length for f=5 c. p. s. Three curves of the lower group were obtained under atmospheric pressure and three curves of the upper group in vacuum.

were obtained under atmospheric pressure and the others in vacuum. As clearly shown in the figure, values of $(S_{a.c})_{f=5}$ for the latter are larger than those for the former, even three or four times larger for short wires, showing that the characteristic a. c. voltage sensitivity is extremely improved by evacuation. This effect is not so conspicuous for larger values of l. This can likely be attributed to the fact that the increase of the time constant by evacuation, for larger values of l, causes the abrupt decrease in the curve of $[1+\omega^2\tau^2]^{-1/2}_{f=5}$ represented as a function of the time constant (see Fig. 2) and as the result, the effect of increase of ε_∞ is lowered.

5. Conclusion

Various thermojunctions were made using old technique for the study of thermojunction characteristics. Examinations under varied conditions led to the conclusion that the performance of thermojunction can be, as pointed out by Hornig and O'keefe, improved by shortening the thermoelectric wire. For example, the time constant of a thermojunction with very short wires ($l=0.15$ mm) was reduced to 0.01 sec. and 0.025 sec. in air and in vacuum respectivery.

As shown in 3, it is desirable to make the heat loss as small as possible without affecting the other characteristics. This is achieved partly by evacuation and partly by reducing the cooling constant, L_r, associated with radiation. The latter is accomplished by narrowing the receiving area, which is also useful in reducing the heat capacity. In fact, in the present experiment, the characteristic a. c. voltage sensitivity was strictly limited by the heat capacity and the radiation loss of the receiver. So $S_{a.c}$ would be still more improved if it be possible to reduce the area of the receiver without sacrificing the external system.

Let us attempt a little more consideration as to the influence of the evacuation upon the time constant and d. c. voltage sensitivity, which in vacuum and under atmospheric pressure are represented respectively by $(\tau)_{vac}$, $(\varepsilon_\infty)_{vac}$ and $(\tau)_{atm}$, $(\varepsilon_\infty)_{atm}$. The value of the ratio $(\varepsilon_\infty)_{vac}/(\varepsilon_\infty)_{atm}$ is 11 for $a_1=50\mu$ and 25 for $a_1=10\mu$, at large l, while that of the ratio $(\tau)_{vac}/(\tau)_{atm}$ is 10 for $a_1=50\mu$ and 18 for $a_1=10\mu$. As assumed previously, if the evacuation merely reduces L without changing any other characteristics of the thermojunction, the ratio for ε_∞ and that for τ should be equal for the same a. It should be noticed that the values for ε_∞ do not actually agree with the values for τ and the disagreement between the values become more pronounced for small values of a_1. Such a fact seems to signify the reduction of the effective heat capacity of thermoelectric wire by evacuation. Fortunately this reduction also causes to increase the characteristic a. c. voltage

sensitivity of the thermojunction.

6. Acknowledgement

The auther wishes to express his gratituds to Dr. Yoshio Fujioka and Prof. Haruo Ootuka for their encouragement and to Prof. Masao Seya for the facilities and valuable discussions given in the present work.

On Optical Properties of Pearl Essence

Sei HACHISU

Institute for Optical Research, Tokyo University of Education

(Received Jan. 15, 1957)

Abstrnat

The size and refractive index of the crystals that constitute pearl essence are measured, and the relation between the luster of pearl essence and the optical properties of the crystal, namely reflection, transmission and scattering are studied.

The crystals are of $(20\sim30\mu)\times(2\sim8\mu)$ rectangles with $70\sim80\,m\mu$ in thickness.

The refractive index is $1.91>n>1.80$.

Theoretical calculation shows that the thickness of the crystal is adequate to the condition for the pearl essence to give out the luster of pearls.

1. Introduction

The pearl essence[1] obtained from the surface of fish scales and of fish bodies, is a kind of special pigment and has a characteristic bright silvery sheen.

It gives out a nacreous sheen when mixed with lacquer or transparent plastic resin, therefore it has been used for the production of imitation pearls and other various substances of nacreous sheen. It is constituted by thin micro crystals of guanin (2-amino, 6-oxi, purin), parallel orientation of which causes the sheen. Several varieties of pearl essences can be obtained from many kinds of fishes, and their qualities—characteristic sheen—are not the same but vary. Nowadays only a few kinds of them are commercially produced, which are those from herring and sardine in America and from tachi-uwo [Tricurus Japonics (Temmink & Schlegel)] in Japan. In this paper, the pearl essence from herring and tachi-uwo is taken up, the former gives out a bright metallic sheen while the latter weak and soft sheen.

2. Crystals constituting the pearl essence

2.1 *Their size and shape*

Fig. 1 is a microphotograph of these crystals, (a) gives the crystals from tachi-uwo, (b) those from herring; crystals in (a) are of nearly $(20\sim30\mu)\times(2\sim3\mu)$ paral-

1) D. K. Stressler: Marine Products of Commerce. New York, Comp. **782** (1923).

lelograms, sides of which are distinct straight lines, while those in (b) are of $(20\sim30\mu)\times(6\sim8\mu)$ long ellipses, margin of which are somewhat faint.

Their thickness is so small that it is impossible to measure by ordinary microscopic technique, but they show characteristic interference colours on their surface, namely gray or white yellow from which we can estimate the optical thickness to be 100 mμ~160 mμ.

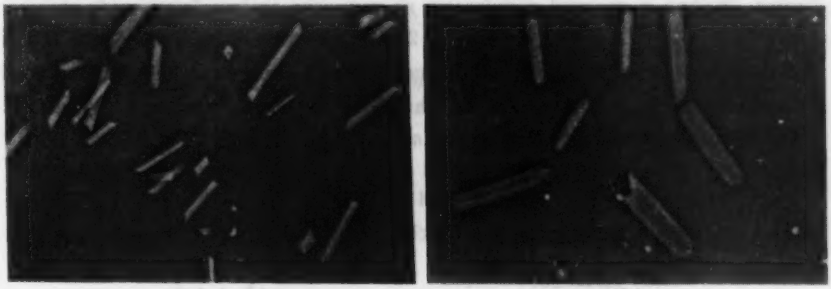

(a) (b)

Fig. 1 Microphotographs of pearl essence crystals
(a) Crystals from Tachi-uwo [Tricurus Japanicus (Temmink & Schulegel)] (500×)
(b) Crystals from Herring (500×)

The thickness can be determined by an interference microscope. It was found to be 70 mμ~80 mμ, as described below.

First of all the crystals are thoroughly cleaned and glued to the surface of a flat plane for observation. The pearl essence is ordinarily preserved in a form of paste made of nitrocellulose mingled with some contaminations partly adhering to the crystal surface. This paste was diluted ten-times with a solvent, such as amyl acetate, and stirred well to make it a smooth lusterous solution. The crystals were then settled by centrifuge and contaminated liquid was removed. After repeating the process 5 times by adding fresh solvent each time on the settled crystals, the final solution was boiled in a flask with reflux condenser for 5 hours. The settled clean crystals were preserved as suspension in a fresh solvent. Crystals so cleaned is of 98% in guanin content.

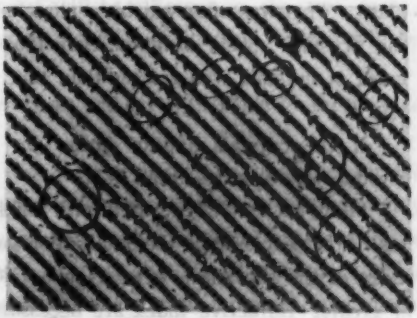

Fig. 2 Pearl essence crystals under interference microscope. Typical samples are marked.

A small drop of this suspension was let fall on the clean surface of a plate glass and evaporated thoroughly to leave the crystals stuck on the surface.

This surface was coated by aluminium by vacuum evaporation and observation was made on photographs taken by an interference microscope. In Fig. 2 white stripes are the crystals and interference fringes crossing over them suffer slight shifts.

From these shifts the thickness of the crystals was estimated; the thickness is given by

$$d=\frac{\lambda}{2}\frac{\Delta l}{l}$$

where λ is the wave length of illuminating light (Na-lamp with $=588\ \mathrm{m}\mu$ was used for measurement), Δl, l represent the shift and the fringe distance. From the photo, $\Delta l/l$ was found to be nearly 1/4, so

$$d\fallingdotseq\frac{588}{2\times 4}=74\ \mathrm{m}\mu$$

Fig. 2 is a photo of the crystals from tachi-uwo. With the crystals from herring, the appearance is almost the same.

2.2 *On the refractive index of the crystals*

For the measurement of refractive index of such small crystals, the immersion method is used, in which the crystals are immersed in a liquid of known refractive index and Becke lines (the bright lines appearing at the rim of crystals) are observed by shifting up and down the focus of the microscope.

In this case the crystals were so thin that the Becke lines were too weak to be recongnized by an ordinary microscope, hence a phase microscope was used, which enabled the detection of the slight difference in refractive index between the crystals and their surrounding.

The crystals were affixed to the sarface of glass as described, on which methylen iodide ($n=1.74$) was dropped to immerse them, and covered with a cover glass. This was observed by a phase microscope of bright contrast which made the crystals appear brighter than their background showing that, the refractive index of crystals was greater than that of methlen iodide, namely greater than 1.74.

If the crystals appear darker by this observation, the refractive index of crystals would be less than 1.74.

Methylen iodide saturated with sulphur gives the refractive index of nearly 1.80. Using this liquid the observation gave also the same result, so that refractive index of the crystals is greater than 1.80. For more precise measurement, liquids of greater refractive index are necessary, but these liquids are all chemically so active that they attack the crystals. So the immersion method can not give neither more precise lower limit nor the upper limit of the refractive index of

the crystals.

For the estimation of the upper limit, a method was devised by the author; it is as follows.

If a thin crystal of refractive index n showing the characteristic interference colour is affixed to the surface of substance of refractive index n′, and observed by a metal microscope, either of two kinds of interference of light would be seen on the crystal surface according to the relation between n and n', namely, when $n>n'$, the phase difference is

(A) $$2\pi\frac{2nd}{\lambda}+\pi$$

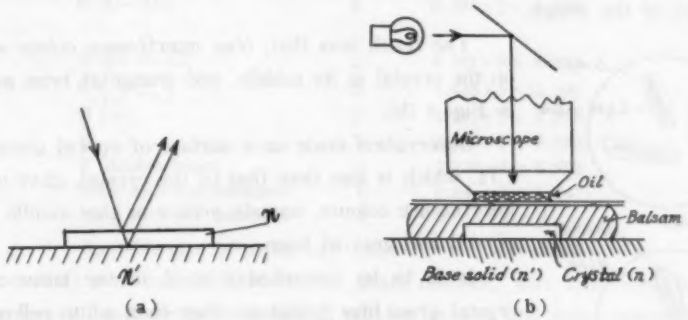

Fig. 3

when $n<n'$, it is

(B) $$2\pi\frac{2nd}{\lambda}$$

where d is the thickness of the crystal.

So the interference colour of the crystal will be different in the two cases; the colour in the former will be the same as observed ordinarily, while it will be different in the latter.

The colours that appear in these two cases are given in Table 1[2] for various values of nd of the crystal.

A transparent block of fused $PbCl_2$ was cracked and on its cleavage surface a small amount of suspension of herring crystals was dropped, dried thoroughly to let the crystals stick on the surface, and observed by a metal microscope. In this case the optical system should be so adjusted that the illuminating light is parallel to the axis of the microscope to realize the normal incidence, and oil im-

2) Hiroshi Kubota: Report of the Institute of Industrial Sience. Unv. of Tokyo **2** No. 6 1952.

Table 1.

case / nd	A ($n>n'$)	B ($n<n'$)
below 30 mμ	dark gray	colourless
30~ 70 mμ	dark gray	white yellow
70~110 mμ	gray	orange
130~136 mμ	light gray	red purple
140~150 mμ	white yellow	purple-blue

mersion method is recommended to remove the stray light harmful for good contrast of the image.

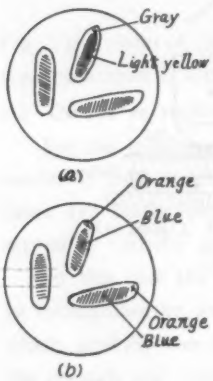

Fig. 4

(a) Crystals from Herring on the glass surface
(b) Crystals from Herring on the lead chloride surface

The result was that, blue interference colour was seen on the crystal in its middle, and orange at brim as shown in Fig. 4 (b).

Observation made on a surface of optical glass of $n'=1.71$, which is less than that of the crystal, gave ordinary interference colours, namely yellow in the middle of the crystal and gray at brim.

It is to be remarked that if in the latter case the crystal gives blue colour or other than white yellow, there is some spacing between crystal and base surface caused by the contamination on the crystal or in the suspension liquid. This is a useful guide to assure the cleaness of the crystal and liquid.

Referring to Table 1 and remembering that nd of the crystal is 100 mμ~160 mμ, it can be said that the case of the crystal on $PbCl_2$ belongs to the case (B) and that on glass to the case (A).

Thus the refractive index of the crystal must be less than that of $PbCl_2$. $PbCL_2$ is a bi-axial crystal, and its main refractive indices are

$$n=2.199 \qquad n=2.217 \qquad n=2.26$$

thus n is less than 2.26.

To obtain more precise upper limit, a special optical glass, index of which is 1.91 (for D-line) was used as the base material. Observation gave the same result as that with $PbCl_2$. so that n is less than 1.91.

Although this method is essencially not precise, because the "dispersion of material" and other complicated phenomena at boundary surface are all left out

of consideration, it can be used for a rough estimation of refractive index of small hin crystals and films.

We can conclude from these experiments that the refractive index of the crystal is greater than 1.8 and less than 1.91.

On the other hand, refractive index is theoreticaly culculated from the molecular refraction as follows.

Structure of guanin is as shown on the right, and its molecular weight is 157. Atomic refractions[3] of component atoms are written down, and sumed up as follows.

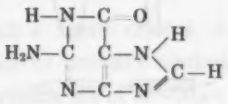

constituting atom	number	atomic refraction
N ($C-NH_2$)	1	$2.322\times1=$ 2.322
N (C—NH)	2	$2.499\times2=$ 4.998
N (C—N=C)	2	$4.101\times2=$ 8.202
C	5	$2.418\times5=$12.090
O (=)	1	$2.211\times1=$ 2.211
H	5	$1.100\times5=$ 5.500
F (double bond)	4	$1.733\times4=$ 6.932
Ring with five members	1	$0.04\times1=$ 0.04
Ring with six members	1	$0\times1=$ 0
R_D (molecular refraction for D-line)		=42.293

The dencity ρ of guanin, that is the pearl essence, was measured by the author by heavy liquid method (mixture of ethylen bromide and ethan tetrachloride) and was found $\rho=1.70$, with which n is culculated from the formula

$$R_D=\frac{n^2-1}{n^2+2}\frac{M}{\rho}$$

This yields $n_D=1.88$.

This value lies between the two limits given by the above experiments. It is appropriate therefore to take $n=1.88$ as the refractive index of the crystals for the present, until more precise measurement is made.

The procedure of above experiments enlightens us to deduce the thickness of the crystals.

As shown in Fig. 4 (b) the herring crystals on the surface of $PbCl_2$ gave interference colours which are blue in their middle, and orange at their brim. The value of nd was determined with reference to Table 1:

$nd\fallingdotseq150$ mμ in middle.

$nd<100$ mμ at brim.

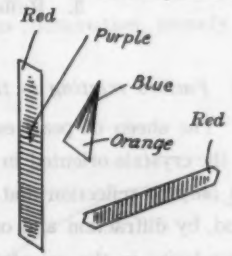

Fig. 5 Crystals from tachi. uwo on the surface of lead chloride.

3) Vorgel: J. Chem. Soc. (1948) 1842.

Fig. 5 shows the crystals from tachi-uwo on lead chloride surface. They are coloured purple uniformly from middle to side except at the ends where the colour is dark red hence the thickness of the crystals is nearly uniform, and is thin at both ends. nd was determined as

$nd \fallingdotseq 140$ mμ for their most part.

$nd \fallingdotseq 110$ mμ at their ends.

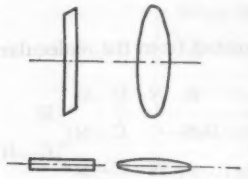

Fig. 6 Cross-sections of crystals (Thickness exaggerated)

Therefore the cross section of the crystal normal to the side line will be narrow rectanglar for tachi-uwo and thin convex lens-like for herring crystal, as shown in Fig. 6.

Results of experiments are arranged as follows.

Table 2.

	Crystals from herring	Crystals from tachi-uwo
Shape	Long ellipse	Narrow parallelogram
Size	20~30μ × 6μ	20~30μ × 3μ
nd in middle	about 150 mμ	about 140 mμ
nd at brim	about 100 mμ	about 110 mμ
d in middle	70 mμ~80 mμ	
n experimental	1.91>n>1.80	
theoretical	1.88 (for D-line)	
specific gravity	1.70	

3. Reflection and Scattering of Light by the Crystals of Pearl Essence

3.1 *Factors relating to the sheen*

The sheen of pearl essence is attributed to the repeated reflections of light by the crystals oriented in lamination. Light incident on the crystals is subjected not only to reflection and transmission but to scattering which is caused, on one hand, by diffraction and on the other, by irregular reflection originating from the irregularity in the orientation of the crystals.

This scattering makes diffuse the reflected light coming out of crystal lamination, and causes the weakning of the sheen.

Hence, the factors relating to the sheen of pearl essence are,

a) Reflection of light by the crystals

b) Scattering by the crystals

1) Scattering due to diffraction

2) Scattering due to irregular reflections

b) 2) is self-evident, and some explanations on a) and b) 1) are given below.

3.2 ***Reflection of Light by the Crystal***

To treat the reflection and transmission of light by such a small crystal, it may seem questionable if these phenomena could be treated by ordinary method applied in the case of infinitely broad thin film. But the crystals are of $20\sim30\mu\times 2\sim8\mu$ rectangle or ellipse, and even the narrowest ones have the breath of 2μ, this being about 4-times of the mean of light wave lengths; hence it will be expected that the ordinary method would give correct results. In the case of normal incidence, the reflectivity of thin film of thickness d is given from the interference theory as

$$R_\lambda(nd)=2\left(\frac{n-n'}{n+n'}\right)^2\left\{1-\cos 2\pi\frac{2nd}{\lambda}\right\} \qquad (1)$$

for monochromatic light, wave length of which is λ; n, n' are the refractive indices of the crystal and surrounding.

As the sheen of pearl essence is observed under the illumination of white light, the reflectivity will be given by integrating $R_\lambda(nd)$ with respect to λ, over the whole region of visible light considering the spector of illumination $E(\lambda)$ and the perceptivity of the eye $V(\lambda)$. It is

$$R(nd)=\frac{\int R_\lambda(nd)\cdot E(\lambda)\cdot V(\lambda)\cdot d(\lambda)}{\int E(\lambda)\cdot V(\lambda)\cdot d(\lambda)}=2\left(\frac{n-n'}{n+n'}\right)^2 Y(nd) \qquad (2)$$

Values of the function $Y(nd)$ were tabled by KUBOTA[3] to obtain the colour diagrams of interference colours of thin film for various illumination, namely for various $E(\lambda)$.

In Fig. (7) $Y(nd)$ is plotted in the case of C-light source illumination. The curve has a maxima at $nd=140$ mμ, namely, the crystal has its maxiumum reflectivity when $nd=140$ mμ.

From the preceding experiments, nd of the crystals of pearl essence are 140m$\mu\sim$ 150 mμ, hence it is concluded that the crystals of pearl essence have a favourable

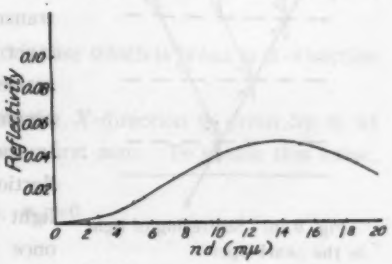

Fig. 7 Relation between the visual reflectivity of thin film and its thickness

value for their maxium reflectivity.

This maximam reflectivity in ordinary vehicle ($n'=1.5$) is culculated postulating $n=1.88$,

$$R(140)=\left(\frac{n-n'}{n+n'}\right)^2 Y(140)=\left(\frac{1.88-1.5}{1.88+1.5}\right)^2 0.99=0.05$$

thus, it is 5% of the incident energy.

3.3 *Scattering of Light by Diffraction*

The diffraction of light by a thin crystal can be divided into two parts, one of which is the diffraction of reflected light and the other is that of transmitted, as illustrated in Fig. 8.

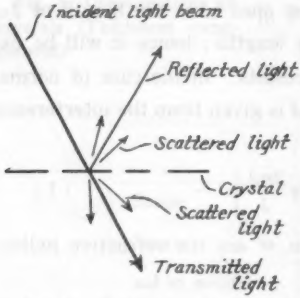

Fig. 8 Scatterring of light by thin crystals

In the following, they are called, for the convienience sake, the reflection scattering and the transmission scattering respectively.

In order to study the manner in which these two kinds of scatterings affect the sheen of pearl essence, the following consideration is given.

The structure of artificial pearl layer made of pearl essence is considered to be as shown in Fig. (9) (a), which, for the sake of simplicity, is modified as Fig. 9 (b) for discussion.

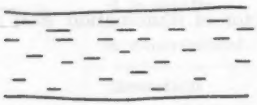

Fig. 9 (a) Structure of pearl layer made of pearl essence

The incident light shown by the bold arrow is subjected, in the pearl layer, to succesive reflections and transmissions, and the scattering occures at every reflection and transmission, so that the incident light pencil becomes diffuse more and more and finally comes out of the layer.

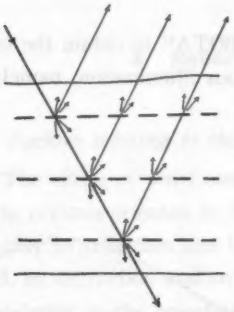

Fig. 9 (b) Scattering of light in the pearl-lager

Speaking in detail, light incident on the crystals jn the first row is partly reflected, and the rest is transmitted; the reflected light comes out of the layer at once accompanied with some reflection scattering, on the other hand the transmitted light accompanied by transmission scattering falls on to the second row to be subjected to further reflection, transmission and scattering. Reflected light from the second row can not come out at once but must pass the first row to suffer once more transmission scattering. Light which passes the second row accompanied by increased scattering will continue repeating the same process.

Thus the reflected light from the pearl layer consists of those coming from the first row, the second row, and so on; the light coming out of n-th row is considered to have suffered 2n-times transmission scattering and only one reflection scattering. From this consideration it may seem that in the reflected light from the pearl layer the transmission scattering would play far more important role than the reflection scattering, but this is not the case, because by the transmission, as will be explained later, only 10% of light is scattered while the whole suffers scattering in the reflection. At all events it may be understood how the two kinds of scattering occur in the pearl layer.

3.3.1 *Reflection Scattering*

The reflection scattering originates from the diffraction of the reflecting light, and it is considered to be equivalent to the diffraction of light passing through a pin hole with the aperture, the area of which is that of the crystal.

It is the case of Fraunhofer diffraction. Coodinates are so chosen as shown in Fig. (10), in which the shape of the crystal is taken to be a rectangle of $(2a \times 2b)$, and z-axis is perpendicular to the crystal surface.

When parallel rays of light are incident in the direction of z-axis, the intersity distrubution of Fraunhofer diffraction is given by the formula.

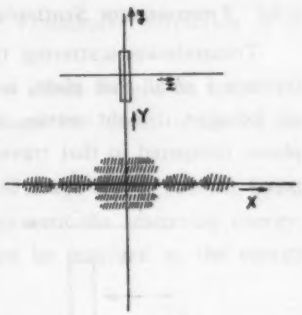

Fig. 10

$$u_{\alpha,\beta} = A_0 \frac{4ab}{\lambda} \left\{ \frac{\sin(ka\alpha)}{ka\alpha} \right\}^2 \left\{ \frac{\sin(kb\beta)}{kb\beta} \right\}^2 \qquad (3)$$

in which A_0 is the intensity of incident light, $k = 2\pi n'/\lambda$, α and β are the direction cosines of diffracted light to x and y axes respectively, λ is the wave length of light and n' is the refractive index of the medium which is the vehicle of pearl essence.

Fig. (10) shows the diffraction pattern in this case which is broad in X-direction and narrow in Y-direction.

The half breadth of zero-order fringe in the X-direction is given by θ_0 at which direction the intensity of diffraction gives first zero. To obtain this value, the conditions

$$\alpha = \sin\theta_0, \quad \beta = 0, \quad u_{\alpha\beta} = 0$$

are substituted in (3), then we have

$$\sin\theta_0 = \frac{\lambda}{2an'}$$

when θ_0 is small, $$\theta_0 \fallingdotseq \frac{\lambda}{2an'} \tag{4}$$

where n' is 1.5 by ordinary vehicles, and for λ 550 mμ is taken. For the crystal from tachi-uwo $2a \fallingdotseq 3\mu$, so the formula results $\theta_0 = 7°$, for the crystal from herring $2a \doteqdot 6\mu$, so $\theta_0 = 3.5°$.

These angles increase when the light comes out of the vehicle to the air to 10° and 5° respectively.

The reflected light is, therefore, more or less diffused, being affected by this diffraction, even if the crystal orientation be complete to reduce thoroughly the irregular reflection. As shown in formula (4) the diffuseness is inversely proportional to the crystal breadth, hence the sheen of pearl essence is expected to be bright or weak according to the breadth of the crystals being great or small.

3.3.2 *Transmission Scattering*

Transmission scattering that originates from the diffraction of light passing through a small thin plate, is dealt with in the theory of phasemicroscope, it is as follows; if light waves passing through the plate suffer a retardation Δ in phase, compared to that travelling the sarounding, they can be considered as composed of two components O and S as shown in Fig. 11 (b), O being the same

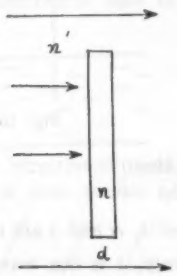

Fig. 11 (a)

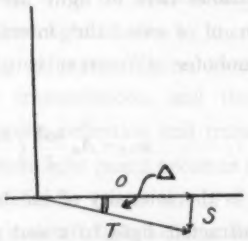

Fig. 11 (b)

as the wave travelling the surrounding and S suffering the retardation of nearly $\pi/2$ in phase. The intensity of S is given by

$$A_s = 2A_0 \sin \Delta/2 \tag{5}$$

where A_0 is the intensity of incident light waves. When Δ is small

$$A_s = 2A_0 \sin \Delta/2 \doteqdot 2A_0 \frac{\Delta}{2} = A_0 \Delta \tag{6}$$

Hence the optical effects due to the existence of the plate are equivalent to those which would be caused by an imaginary light S supperposed on the uniform back ground of incident light and passed through a pin hole with the aperture, the area of which is that of the plate.

As Δ is given to be

$$\Delta = 2\pi \frac{n-n'}{\lambda} \cdot d \tag{7}$$

the intensity of S is

$$A_s = A_0 \Delta = 2\pi \frac{n-n'}{\lambda} \cdot dA_0$$

and its energy is

$$|A_s|^2 = 4\pi^2 \left(\frac{n-n'}{\lambda} \right)^2 \cdot |A_0|^2 \cdot d^2$$

The scattering ratio is

$$\frac{|A_s|^2}{|A_0|^2} = 4\pi^2 \left(\frac{n-n'}{\lambda} \right)^2 \cdot d^2 \tag{8}$$

hence it is proportional to the square of d.

As in the case of the reflection scattering, the Fraunhofer diffraction of S waves cause the transmission scattering.

If a convex lens is placed behind the plate, the image formed on the forcal plane consists of the diffraction pattern of S waves and the point image of the uniform light O waves.

The diffraction pattern is overlapped on the point image of the uniform light. Hence the whole energy of S waves do not truly represent the scattering energy, but it is a dominant factor of the scattering and can be regarded as the energy of the scattering for approximation.

This scattering causes the diffuseness of transmitted light.

The scattering ratio is plotted in Fig. 12 with respect to d and $\frac{2\pi}{\lambda}\Delta$, where $n=1.88$, $n'=1.5$ are taken; and when $d=74\,\mathrm{m}\mu$—$nd=140\,\mathrm{m}\mu$—, namely when the reflectivity is maximum, the ratio is 0.1; namely 10% of transmitted light is scattered.

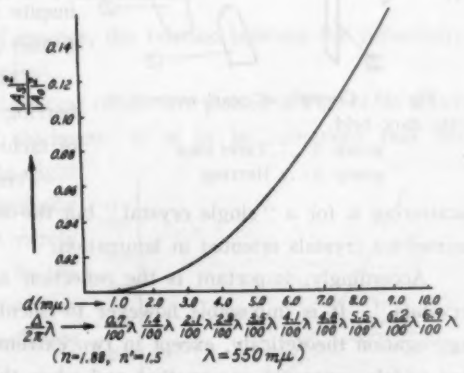

Fig. 12

The angular distribution of diffracted S waves are exactly the same as that of reflection scattering because both are postulated to be equivalent to the diffraction of light by a pin hole.

If the size of crystal becomes large, most of diffracted light concentrates into

the center of zero-order fringe, thus the scattering is substantially decreased; that is, the sheen of pearl essence will become sharp and intense, as concluded in the section of the reflection scattering.

The above discussion is for the crystal with uniform thickness, but the natural crystals are never uniformly thick, but thick in middle and thin at brim or at ends, as described before. In such a case diffracted light tends to concentrate into the middle of zero-order fringe.

This effect is easily observed by a microscope with Cardioide condenser, field through which is dark suitable for observation of scattered light.

The appearance is sketched in Fig. 13; crystals from tachi-uwo give intense bright lines at their rim, while those from herring give weak lines except at broken edges where intense lines appear.

In order to examine closely the effect of the brim thickness, it is necessary to compare two crystals which are equal in thickness and breadth, differing only in brim thickness, because the scattering is, as described before, depend also upon the breadth.

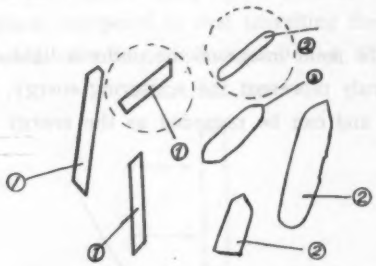

Fig. 13 Crystals of pearl essence in the dark field
group ①....Tachi-uwo
group ②....Herring

Very narrow ones of herring crystals have breadths almost equal to those of tachi-uwo; and the former is thicker than the latter as described before.

Fig. 13 shows that bright lines of the former are weaker than those of the latter inspite of greater middle thickness of the former; two samples are marked by circles.

This explains well that the sheen of herring pearl essence is brighter than that of tachi-uwo.

Preceding study on the reflection and scattering is for a "single crystal" but the sheen of pearl essence is produced by numerous crystals oriented in lamination.

Accordingly, important is the reflection and scattering by "aggregation of crystals". It is impossible however to calculate the interference effects of such aggregation theoreticaly, except in two extreme cases, namely when the crystals are widely seperated one another and when they are close together piled on face to face.

In the former case the resultant is the arithmetical sum of the components, while in the latter it is essentially equivalent to the effect of the "single crystal" of multiple thickness. For instance, when two crystals come to contact face to

face, the thickness is doubled, so it readily follows from farmula (8), that scattering increases 4-times, namely twice as much of the sum of two seperate scattering, while the reflectivity remains unaltered. This explains the fact that the pearl essence lose its sheen when its component crystals coagulate by some reason.

In the use of pearl essence as applied for making imitation pearl to give pearl luster by coating, the crystals are so oriented as the spacing between them is of the order of light wave length, while in the case of being mixed in resin, the spacing is about 1/100 mm. Thus the resulting scattering will be varied from the said extreme case in which the caystals are widely seperated, and it will be different by the kind of application.

From experience it is known that pearl essence gives out brighter sheen when it is used in resin work than in coating. This fact seems to indicate the existence of interference effects causing the greater scattering in the case of coating by which crystals laminate closely.

But the irregularity of spacing will dull the over-all interference effects, whereby the reflection and scattering will be treated approximatly as the arithmetical sums of respective components. Only on this assumption, we can deduce the sheen of pearl essence from the reflection and scattering of single crystal, and as will be discussed later it gives satisfactory results.

4. Sheen of Pearl Essence

To account for the sheen of pearl essence, the relation between the reflectivity and the scattering ratio must be studied.

Two curves —reflectivity and scattering ratio— are plotted in Fig. 14, in which the abscisa represents the crystal thickness. It is to be remarked that the reflectivity is calculated for white light (C-light source) considering the perceptivity of the eye, while scattering ratio is merely for monochromatic light of 550 mμ. So the use of the curves in this Fig. is not correct for precise investigation but will be sufficient for approximate estimations.

The Fig. shows that the reflectivity has a maximum at $d=74$ mμ, while the scattering increases rapidly.

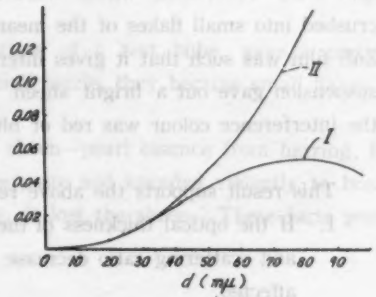

Fig. 14
I....Reflectivity–Crystal thickness curve
II....Scattering–Crystal thickness curve

As described before, the crystals of pearl essence have the thickness of 70–

80 mμ, namely they have a suitable thickness for great reflectivity and the fact that the rate of increase of scattering is not large for the thickness below the above value, and that crystals are thin at brim in the case of herring, favours to lessen the transmission scattering.

Thus it is concluded that the crystals of pearl essence have a favourable thickness for great reflectivity and relatively small scattering, namely for good sheen.

If the crystal thickness becomes over 80 mμ, from middle to brim, the reflectivity would decrease and the transmission scattering increase rapidly, resulting in a small reflectivity and much scattering, so that the pearl essence could hardly give out sheen.

But strictly speaking, conclusive explanation can not be given for the cause of the sheen of pearl essence merely from the above consideration, since the conditions to give out sheen described above may not be sufficient on account of the above discussion being too vague to derive mathematically the intensity of reflection, the angular distribution of which is fundamental to explain the cause and brightness of the sheen.

Some experiments were made to support and supplement the foregoing reasoning.

Experiment 1.

A substance similar to pearl essence in appearance was produced from a thin film.

A thin film of ZnS was made on a collodion film by vacuum evaporation. This collodion film was put into amyl acetate and collodion was dissolved leaving ZnS film. Ultra-sonic waves were applied to it, and ZnS film in the liquid was crushed into small flakes of the mean size of 1/100 mm. When the thickness of ZnS film was such that it gives interference colour of gray or white yellow, this suspension gave out a bright sheen. Whereas, with the thickness with which the interference colour was red or blue, the suspension appeared dull.

This result supports the above reasoning which gives some corollaries, namely

1. If the optical thickness of the crystals is less than 140 mμ, the reflectivity and scattering ratio decrease parallel, so the resultant sheen will not be affected.
2. If the crystals are large enough for the diffracted light to be concentrated into the center of zero-order fringe, lamination of such crystals will give

out a sheen regardless to the thickness of the crystals, but on the contrary, if the crystals of pearl essence with bright sheen are crushed into small specks, the essense will lose its sheen. These corollaries were proved by the following experiments.

Experiment 2.

To prove corollary 1, very thin film must be prepared. ZnS film, if it is very thin, breaks up in powder when dipped into solvent to dissolve collodion membrane on which ZnS is deposited. Basic lead carbonate crystals were found suited for the purpose. Crystals in the form of hexagonal thin plate of approximately 1/100 mm in size are obtained by passing CO_2 gas through a dilute solution (0.01 mol) of lead acetate. The thickness of the crystal can be controlled by the condition of reaction. Two kinds of crystals were prepared, both resembling to pearl essence with bright sheen as theoretically expected, the optical thickness (nd) being below 100 mμ for one and approximately 140 mμ for the other. The optical thickness was estimated by the method described in page 24. The sheen of the former was a little softer than that of the latter due probably to increased amount of irregular reflection, for greater numbers of thinner crystals are necessary to give the same intensity of reflection as that by thicker crystals and hence the irregular reflection will be multiplied.

Experiment 3.

The relation between the crystal size and the sheen was made clear as follows; crystals of lead thio-sulfate of 1–2 mm in size and more than 200 mμ in optical thickness showing beautiful interference colours, were prepared by mixing equal amounts of lead acetate solution of 1/100 mol and hypo of the same concentration, at 50°C.

These crystals when settled on the bottom of a test bube, gave a metalic bright sheen, and when forced out of a small nozzle, they became small flakes of 1/100–5/100 mm in size, and lost the sheen.

The natural pearl essence with bright sheen—pearl essence from herring, for instance—if mixed with thick nitrocellulose paste and kneaded violently to break it up into small specks of 2–4μ in size, it lost the sheen. These facts prove corollary 2.

Summary

The size, thickness and refractive index of the crystals of pearl essence were

measured. Conclusion is given that the size and thickness are correct to cause the bright sheen.

Acknowledgement

The auther wishes to express his sincere thanks to Prof. Y. FUJIOKA[4] for his kind instruction and also to Dr. H. INUGAI[5] for his helpful advise in chemistry. Thanks are also due to Dr. M. IWATA[6] for his help in the experiment of ZnS film.

4) Present position Member of the Japanese atomic energy committe.
5) Instructor of, faculty of engineering, Meiji University.
6) The Osaka industrial resarch institute.

Spectroscopic Studies on the Interaction Between Indole, Carbazol and Aromatic Hydrocarbons

Yoshiki SATO

Institute for Optical Research, Tokyo University of Education

(Received Dec. 15, 1957)

Abstract

The first overtone bands of amino stretching vibrations of indole and carbazole in dilute solutions of aromatic hydrocarbons are measured by using a near infrared spectrometer with a great resolving power, correlations of which with the ionization potentials and basic properties of the aromatic nuclei are discussed. Further, based on these relations, interaction between the solute and the solvent molecules is also described.

1. Introduction

In recent years, studies on the basic properties of aromatic hydrocarbons have been made. In particular, Benesi and Hildebrand[1] gave a considerable attention to the fact that the postulated basic natures of aromatic nuclei are closely connected with the absorption spectra in the ultraviolet region which arise from iodine-aromatic complexes, and that the presence of such complexes appears possible to be explained on the basis of an acid-base interaction. Andrews and Keefer[2] suggested that the magnitude of the equlibrium constants for the formation of $ArAg^+$ which are obtained from the solubilities of certain aromatic hydrocarbons and substituted benzenes, may be considered as a measure of the basic strengths of the aromatic rings. Recently, Brown and Brady[3] examined the dissolution of hydrogen chloride at $-78.51°$ in dilute solutions of aromatic hydrocarbons in toluene and in n-heptane, and ascribed the solubilities of hydrogen chloride to the basic characters of the aromatic nuclei in question. More recently, Andrews and Keefer[4] also estimated the equlibrium constants for various polymethylbenzene complexes of iodine and iodine monochloride, using the ultraviolet absorption methods. But among the data listed by these workers it seems there are more or less discrepancies.

1) H.A. Benesi and J.H. Hildebrand: J. Am. Chem. Soc. 70 (1948) 2832; 71 (1949) 2703.
2) L.J. Andrews and R.M. Keefer: J. Am. Chem. Soc. 71 (1949) 3644; 72 (1950) 5034.
3) H.C. Brown and J.D. Brady: J. Am. Chem. Soc. 74 (1952) 3570.
4) L.J. Andrews and R.M. Keefer: J. Am. Chem. Soc. 74 (1952) 4500.

In the previous paper[5], it was shown that the wavelengths of phenol hydroxy. stretching bands in several diluted aromatic solutions increase with decreasing ionization potentials of the aromatic compounds, on the basis of which the stability of loose complexes formed by the aromatic nuclei with phenol was discussed as due to the ability of the aromatic ring to accept the proton from the reagent. Since the ionization potentials of aromatic compounds should be a measure of the relative tendency of the aromatic nuclei to function as bases, it therefore appears desirable to correlate the wave number of such absorption bands as just described above with the basic properties of the aromatic nuclei.

For the purpose of studying this problem in the present investigation which represents an extenction of the work reported previously, indole and carbazole amino stretching vibration bands have been observed in dilute solutions of various aromatic hydrocarbons, using a near infrared spectrometer with a great resolving power, outlined in the previous paper. As a result, it has been obtained that the wave numbers of the absorption bands are, as noticed for phenol, closely related to the ionization potentials and the basic strengths of the aromatic nuclei.

2. Experimental and Results

The first overtone bands of amino stretching vibrations of indole and carbazole, the fundamental bands of which in benzene solution were observed previously by Josien et al[6]., were measured by means of the near infrared spectrometer, in dilute solutions of the following aromatic hydrocarbons: benzene, toluene, o-, p-xylenes, mesitylene, ethylbenzene, isopropylbenzene and t-butylbenzene. For special purposes, carbon tetrachloride was also used as solvent. Most of these compounds are commercial products, prepared purest available. The rest were redistilled before being used. All the spectral measurements were made at a room temperature in a concentration range from 0.005 mole/1. to 0.04 mele/1. for both indole and carbazole, in such a concentration no band associated with hydrogen bonding between the solute molecules being observed. The cell thicknesses are 1.5 cm. to 3 cm.. Since the absorption bands observed are so broad that it seems somewhat difficult to determine the exact wave numbers of these absorption maxima, their possible numbers by approximate estimation are collected in Table 1.

5) Y. Sato: Science of Light [Tokyo] 5 (1956) 49.
6) N. Fuson, M-L. Josien, R.L. Powell and E. Utterback: J. Chem. Phys. 20 (1952) 145.

Table 1. Wave numbers of the first overtone bands of NH stretching frequencies of indole and carbazole, wave number shifts (in reference to wave numbers in carbon tetrachloride), and ionization potentials and relative basic properties of the aromatic hydrocarbons.

Solvent	ν^a	$\Delta\nu$	ν'^a	$\Delta\nu'$	I_p	Relative basicity (HCl)	Relative basicity ($ArAg^+$)
Benzene	6764	82	6742	89	9.24[b]	0.61	2.41
Toluene	6752	94	6729	102	8.82[b]	0.92	2.95
Ethylbenzene	6743	103	6720	111	8.77[c]	1.06	2.7
Isopropylbenzene	6740	106	6716	115	8.76[c]	1.24	2.8
t-Butylbenzene	6738	108	—	—	[d]	1.36	2.3
o-Xylene	6735	111	6713	118	8.58[c]	1.13	2.89
p-Xylene	6733	113	6711	120	8.48[c]	1.00	2.63
Mesitylene	6698	148	—	—	[d]	1.59	1.8

a) Primed and unprimed are related to indole and carbazole respectively.
b) K. Watanabe: J. Chem. Phys. 22 (1954) 1564.
c) V.G. Hammond, W.C. Price, J.P. Teegan and A.D. Walsh: Discuss. Faraday Soc. No. 9 (1950) 53.
d) See reference (12).

3. Discussions

All of the NH absorption bands obtained in dilute solutions of the aromatic hydrocarbons possess two broad yet nearly completely separated peaks. Such a splitting of absorption band has already been pointed out by several workers[7)-9)], for the cause of which a few interpretations have been made. In order to obtain more definite evidence to justify Jones and Badger's proposal, in which the higher frequency component is considered as arising from molecules free from the solvent association, the NH absorption bands of indole were measured in mixed solvents containing benzene with different ratios to carbon tetrachloride. As a result, it was found that as the ratio increases, i.e., dielectric constant or index of refraction of the mixed solvent becomes larger the wave number of the higher frequency component decreases from the value obtained in carbon tetrachloride solution towards that obtained in benzene solution, while the position of the lower frequency component remaines almost unchanged. Such a fact clearly tends to support the previously mentioned Jones and Badger's explanation for the experimental results. Thus the wave numbers listed in Table 1 are of the lower frequency

7) R. Mecke: Disc. Farady Soc. No. 9 (1950) 161.
8) H. Jones and R.M. Badger: J. Am. Chem. Soc. 73 (1951) 3132.
9) S. Searles and M. Tamres: J. Am. Chem. Soc. 73 (1951) 3704.

components originated from the solute molecules associated with the solvent molecules.

As described in the previously cited paper[5], the loose complex may likely be considered as due to weak interaction between the π electrons of the rings and the NH bond of indole or carbazole, and it seems to correspond to the π complex which has been proposed by Dewar[10] as intermediate in aromatic substitution reaction, or, the π-complex first suggested by Brown and Brady in their paper[3]. In such a complex, the resonance energy, which is due to electron migration from the highest occupied orbital of the aromatic ring mainly to the antibonding orbital of the NH σ bond, appears to play an important role in strengthening the bond, on which non-resonance energies are superimposed. However, it is considered that the resonance energy, in other words, the donor strength of the aromatic nuclei is not large as inferred from the estimated equilibrium constant for the several phenol-aromatic complexes using ultraviolet absorption method[5]*. Accordingly, the potential barrier for the proton transfer in such a weak hydrogen bonding would be considered so high that no splitting of lower levels occurs[11].

As seen in Table 1, the wave numbers of the NH stretching bands of both indole and carbazole, as is the case of phenol, are closely related with the ionization potentials of the aromatic molecules, the order of which adopted here from various values measured by several investigators is such as to agree with that calculated by Franklin[12] using an united atom model, and also as inferred partially from the capacity of the substituent group, through inductive or hyperconjugation, to increase the electron density of the aromatic nucleus. If for binding energy of these complexes the above-mentioned interpretation is allowed, such an excellent relationship may easily be understood. Further it appears that according to the conditions advanced by Dewar[13], which influence upon the strength of base, the relative stability of the complexes formed by various aromatic hydrocarbons with indole or carbazole should be a measure of the relative basic properties of the aromatic nuclei, since in such a complex the electron donor molecule

* The eqilibrium constant, for example, for phenol-benzene complex was estimated as 1.5 by the ultraviolet absorption study, which is also in good agreement with 1.4 obtained from the infrared absorption method. Then the ultraviolet spectra described in the previous paper are, as already pointed out, necessarily interpreted as arising from the complex. The equilibrium constant for the indole-or carbazole-aromatic complexes would be considered to be nearly of the same order as above.

10) M.J.S. Dewar: J. Chem. Soc. 406 (1946) 777.
11) Y. Sato and S. Nagakura: Science of Light [Tokyo] 4 (1955) 120.
12) J.L. Franklin: J. Chem. Phys. 22 (1954) 1304.
13) M.J.S. Dewar: The Electronic Theory of Organic Chemistry, (Oxford University Press, 1949).

accormodates the electron acceptor possibly without the sacrifice of appreciable resonance energy. Remenbering that the wave number shift can usually be regarded as a measure of the stability of the complex, the wave numbers of the NH absorption band of indole or carbazole in the diluted aromatic solutions seem to offer a direct means to determine the relative basicity of the aromatic nuclei.

Of late, the basic characters of the aromatic hydrocarbons have been discussed by several investigators. In order to compare with the observed data, in particular, the relative basicities obtained by Brown and Brady[3] are listed in the seventh column of Table 1, and the equilibrium constants for argentation of the substituted benzenes given by Andrews and Keefer[3] in the eighth column. These are in good agreement with a few exceptions. The order of the relative basic strengths of the methylated benzenes is benzene<toluene<xylene<mesitylene, which would be predicted from the fact that a methyl substituent enhances slightly the electron density of the benzene ring, as reflected in the values of the ionization potentials for benzene and methylated benzenes, since, in the usual aromatic hydrocarboms, both of hyperconjugation and inductive effect of substituent groups produce a raising of the highest occupied orbital of the substances. The anomaly of the order of the equilibrium constant for mesitylene was explained by Andrews and Keefer on the basis of steric hindrance of the methyl groups opposing the silver-ion complex.

In o-, p-xylenes, the observed order of the relative basic strength, even though the grading is flat, is reverse compared with that given by other workers. However, considering the larger ionization potentials of p-xylene, it would be reasonable to expect that the donor strength of p-xylene is over that of o-xylene. This discrepancy may be explained as due presumably to the steric repression of the two methyl groups opposing the complex formation, but, it appears doubtful whether such an interpretation is applicable for the reversal of the relative order of basicities shown by Brown and Brady. The observed order of the alkylbenzenes in the relative base strength is toluene<ethylbenzene<isopropylbenzene<t-butylbenzene in excellent agreement with the result obtained from the solubility of hydrogen chloride, while in comparatively poor correspondence to the order predicted from the σ values given by Hammett[14] for these alkyl groups, which is also related to closely similar modifications of the ring electron distributions brought out by the alkyl groups. The discrepancy of the latter seems probably due to the fact that the σ constant is referred to a physical situation influenced by polarizing effects of reacting group inducing large changes in the electron

14) L.P. Hammett: Physical Organic Chemistry, (McGraw-Hill Book Company, Inc., New York, 1941).

distribution. The above fact leads us to conclude that in these alkylbenzenes the capacity of the alkyl groups to hyperconjugate with the aromatic nucléus is inferier to that of inductive effect of these groups, as reflected on the ionization potentials.

Based on the fact that the wave numbers of indole or carbazole in dilute solutions of the aromatic hydrocarbons appear likely, as indicated above, to be influenced only by the ionization potentials of the aromatic nuclei, with Dewar's kinematical investigation[13] for the base strength in mind, we reach to the following conclusions; the wave number in question seems unlikely to be influenced considerably by such other factors as the steric effect and the polarizing effect. Accordingly the solute molecule, in the complex, is bound, mainly on the resonance energy due to delocalization of the π electrons of the aromatic nuclei, nearly perpendicular to the plane of the benzene ring on the symmetrical axis.

Aknowledgment

The author sincerely thanks to Professors Yoshio Fujioka and Haruo Ootsuka for their deep interest and constant encouragement, to Prof. Masao Seya for his advice and facilities, and to Dr. S. Nagakura, University of Tokyo, for his guidance and encouragement. Thanks also are expressed to Assit. Prof. Sei Hachisu for his facilities and to Mr. Sanzo Takezawa for his valuable aid in the experimental work.